Chemical vapour deposition of oriented diamond nanocrystallites by a bias-enhanced nucleation method

Chemical vapour deposition of oriented diamond nanocrystallites by a bias-enhanced nucleation method

Jhih-Kun Yan and Li Chang

Department of Materials Science and Engineering, National Chiao Tung University, 1001, Tahsueh Road, Hsinchu 300, Taiwan, Republic of China

E-mail: zhikun.mse91g@nctu.edu.tw

Abstract
A microwave plasma chemical vapour deposition (MPCVD) system has been used to deposit nanometre-sized single-crystalline diamonds on 1×1 cm^2 Si(100) substrates. The distribution of deposited diamonds has good uniformity over the whole Si substrate surface by using a dome-shaped Mo anode which allows the application of bias-enhanced nucleation. The morphology and crystallinity of the deposits on Si were characterized by scanning electron microscopy (SEM) and transmission electron microscopy (TEM) with electron diffraction and lattice images. SEM and TEM observations show that oriented diamond nuclei as single crystals with facets can form on self-formed Si cones through epitaxial SiC within a short bias period. After a longer bias time, it has been observed that polycrystalline diamonds formed as a result of secondary nucleation.

1. Introduction

The synthesis of diamond has attracted much attention in the past few decades, owing to its outstanding properties, such as chemical inertness, a wide band gap, excellent biological compatibility, and the greatest hardness and thermal conductivity [1–3]. In recent years, the fabrication and applications of nanostructured materials has been one of the research topics most focused on, because of their unusual physical properties [4–6]. Nanocrystalline diamond has been proved to be a candidate for optical, electronic, and mechanical devices because of its unique properties, such as low optical absorption coefficient, good field emission efficiency, and adhesion to substrates [7–11]. Gruen *et al* [7] first reported the nucleation and growth of nanocrystalline diamond films on scratched Si substrates. Also, the study of single nitrogen–vacancy (N–V) centres in diamond has attracted much attention in the field of quantum optics [12–15].

Nanocrystalline diamond has already been synthesized by using the chemical vapour deposition (CVD) method, however the diamond often appears as disordered crystals or in cauliflower-like shapes in the film structure of diamond, which contains high densities of defects such as grain boundaries,

stacking faults and five-fold twins [10, 16–18]. It is rarely reported that nanocrystalline diamond is of regular shape with low defect density. Actually, it is of interest to synthesize defect-free and single-crystalline nanodiamond not only for its applications in nanotechnology but also for the scientific study of the properties on the nanometre scale.

Bias-enhanced nucleation (BEN) has been a widely used method to increase the nucleation density of diamond on a mirror-polished silicon substrate in a CVD system through ion bombardment [19, 20]. It is a common practice for the growth of heteroepitaxial layers [21]. However, the BEN process involves spatial and temporal evolution of the bias discharge consisting of the superposition of a microwave plasma with a modified dc glow discharge [22–26]. As a result, uniform deposition of diamond is difficult to obtain using the BEN method.

In this work, we used a microwave plasma chemical vapour deposition (CVD) system to deposit diamond. The distribution of microwave plasma and dc glow discharge has been improved by using a Mo anode to deposit uniform diamond nuclei on a Si substrate. As a result, the arrays of nanometre-sized diamonds that are uniformly distributed over all the Si substrate surface can be deposited in a short bias time.
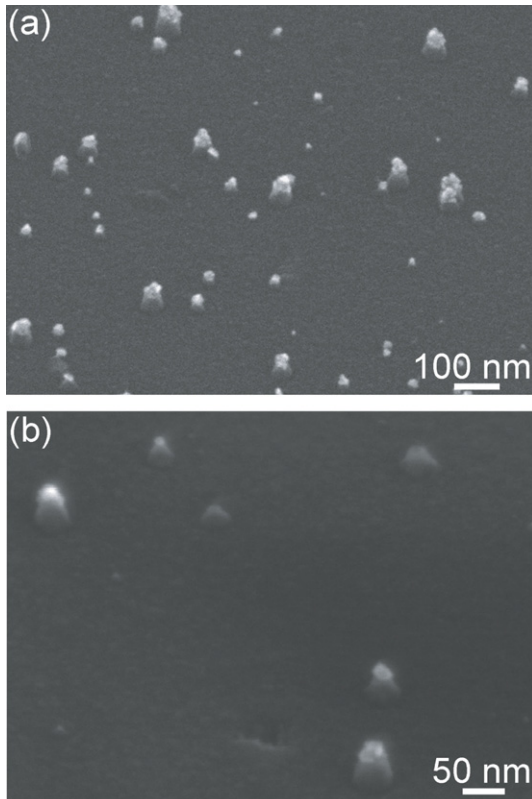
Figure 1. (a) SEM image of cone-like particles synthesized using a 5% CH_4 concentration for 1 min. (b) A high-magnification view of (a).

Most of the diamonds are single crystalline, with a rhombus-like shape growing along the Si[100] direction. Also, the evolution of diamond crystallites formed in the early stage is discussed, based on characterization by electron microscopy.

2. Experimental details

The deposition of diamond was carried out in an ASTeX-type microwave plasma CVD system. In order to optimize the microwave discharge and extend the bias-induced discharge over the whole substrate, we designed a dome-shaped Mo anode with a diameter of 15 mm which was located above the substrate as a counter-electrode and the distance between the disk anode and substrate was varied in the range from 15 to 30 mm. The schematic diagram of the apparatus has been described elsewhere [27]. Mirror-polished p-type (100) silicon wafers with dimensions of 1×1 cm^2 without any mechanical pre-treatment were used as the substrate. Before deposition, the substrate was etched in 1% hydrofluoric acid in de-ionized water for 60 s and ultrasonically cleaned with acetone for 10 min. The substrate was then placed on a Mo-disk holder. The deposition process consisted of heating and biasing stages. In the heating stage, a hydrogen plasma with the addition of 2% CH_4 was initially applied to the substrate for 10 min to raise the substrate temperature to the required degree of about 800 °C and to clean the substrate surface. The substrate temperature was monitored by an optical pyrometer. For biasing, a voltage of -100 V was applied to the substrate for 1 min with 5% CH_4. The detailed processing parameters for the heating and biasing stages are as follows: the total gas
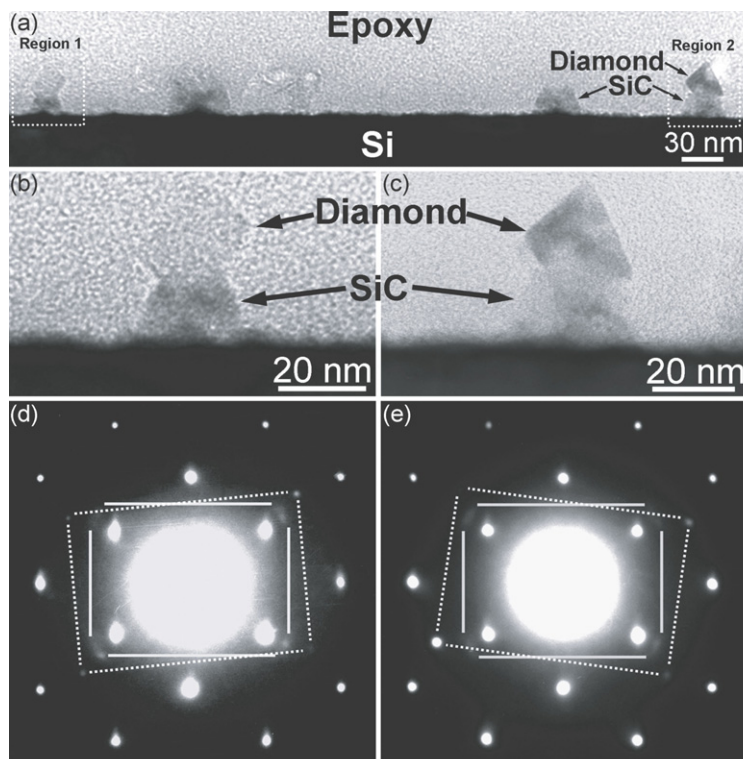

Figure 2. (a) Cross-sectional bright-field TEM showing the cone-like structure on a Si(100) substrate. (b) and (c) High-magnification view of the marked regions 1 and 2 in (a), respectively, and (d) and (e) the corresponding selected area diffraction (SAD) patterns in the Si[011] zone axis shown in (b) and (c), respectively, showing typical diamond {111} and cubic SiC{111} reflections.
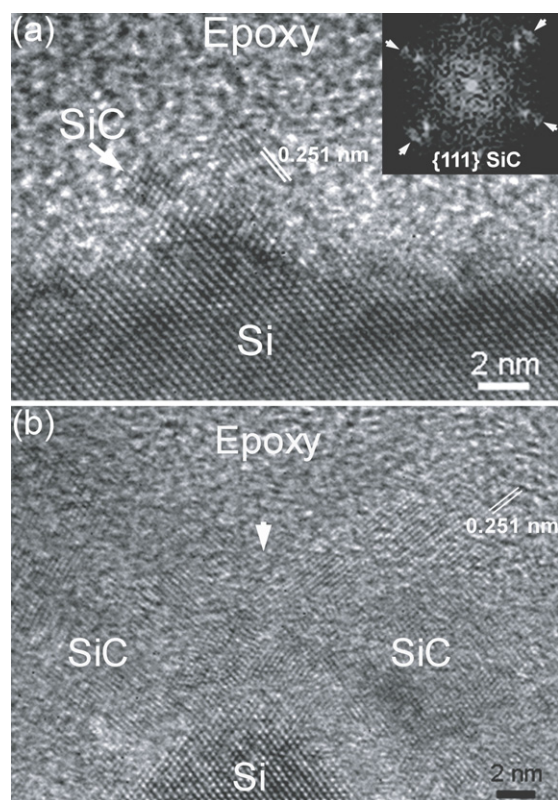
Figure 3. (a) HRTEM image of a cone without diamond on top, with the inset the FFT pattern, showing SiC epitaxial to the Si cone. (b) Another case with a bigger Si cone, showing the formation of a grain boundary between both SiC crystals.

pressure was 20 Torr, the microwave power was 800 W, and the total flow rate was 300 sccm. After the biasing process, the surface morphology was examined using a JEOL JSM-6700F field-emission scanning electron microscope (SEM). The microstructure of the deposits was further characterized in a Philips Tecnai 20 transmission electron microscope (TEM). High-resolution transmission electron microscopy (HRTEM) was performed in a JEOL-2100F microscope for interface characterization.

3. Results and discussion

After a 10 min heating and cleaning procedure in the hydrogen–carbon plasma, the surface, as characterized by atomic force microscopy, is smooth with a root-mean-square (rms) roughness of ~0.25 nm. The HRTEM analysis (not shown) also shows that the surface is smooth and no diamond can be found. The results indicate that the heating stage does not lead to any diamond nucleation and the smooth surface can be a good ground for the following bias stage.

Figure 1(a) shows the surface morphology of the deposits on a Si substrate after the bias. The deposits on the surface exhibit a cone-like shape, and the estimated density of the deposited particles is about $4 \times 10^9 \mathrm{cm}^{-2}$. The base diameter of cone-like particles is roughly in the range of about 10–60 nm, with an average of ~30 nm. The image contrast of the cone-like particles shows that the top region is bright,

whereas the rest is dark. In fact, the top bright regions are of diamond crystals, as shown in TEM. The diamond size is smaller, with an estimated average of ~20 nm. Some cones are covered with a number of randomly distributed diamond crystals with a size of a few nanometres, while it can be observed that a large fraction of cones seems to be topped with faceted single diamonds, as shown in a high-magnification SEM image in figure 1(b). It is also noticed that the diamonds only form on the tip, not around the base and the sides of the cones. The results mentioned above are also supported by TEM observations (figure 2).

Figure 2(a) is a bright-field TEM micrograph which shows the cross-sectional view of the deposited crystals on the Si substrate. The rhombus-like diamond crystals with facets can be seen clearly at the top of the cones, similar to the SEM observations. Figures 2(b) and (c) are high-magnification views of regions 1 and 2 in figure 2(a), respectively. These two images show similar morphology, with the same structures consisting of diamond, SiC and Si as shown in figures 2(d) and (e) of the corresponding selected-area diffraction (SAD) patterns along the Si[011] zone-axis, respectively. From SAD, diamond facets are probably parallel to {111}. Although there are several cones in the field of view, the SAD patterns reveal that all the cones are oriented along the substrate normal of [001] with the same crystallinity characteristics. The reason for the formation of the Si cone is not well understood at the moment; thus, further investigations are under way. In the SAD patterns, cubic SiC{111} spots can be identified and are in registration with silicon {111} spots, suggesting that the cubic SiC is epitaxial to Si. The diamond spots can also be identified. As there are no randomly distributed diamond reflections, it may imply that there exists a single-crystal diamond on each Si cone. The statistics from examinations of several tens of cones in the same TEM specimen in figure 2(a) show that about 50% of the cones are topped with a single diamond similar to those shown in figure 2. Interestingly, it is also found that some of the cones do not show diamonds on the tips, as shown in figure 2(a).

To clarify the relationships between diamond, SiC, and Si phases, HRTEM analysis was performed. All of the following HRTEM images were taken from different areas in the same TEM specimen for the examination of figure 2(a). Figure 3 shows the case without any diamond on top. From lattice fringes and the fast Fourier transform (FFT) pattern, it is shown that two SiC crystallites epitaxially form on opposite sides of the Si cone, resulting in a (volcano-like) V-shaped groove at the Si tip. Also, it is observed that each SiC has {111} facets. In figure 3(b), another case with a larger size than that of figure 3(a) shows the growth of SiC, which results in the formation of a grain boundary between both SiC crystals misoriented with each other, as marked by a white arrow. The misorientation is probably caused by the planar defects and dislocations. Nevertheless, the V-groove persists with SiC growth.

Figure 4(a) is an HRTEM image taken from an Si cone topped with a diamond crystal which grew on SiC. Figure 4(b) is an enlarged view of the region around the black arrow in figure 4(a), showing the interfacial area between the diamond and SiC. Both lattice fringes of SiC{111} (spacing of 0.25 nm) and diamond {111} (spacing of 0.206 nm) can clearly be seen.
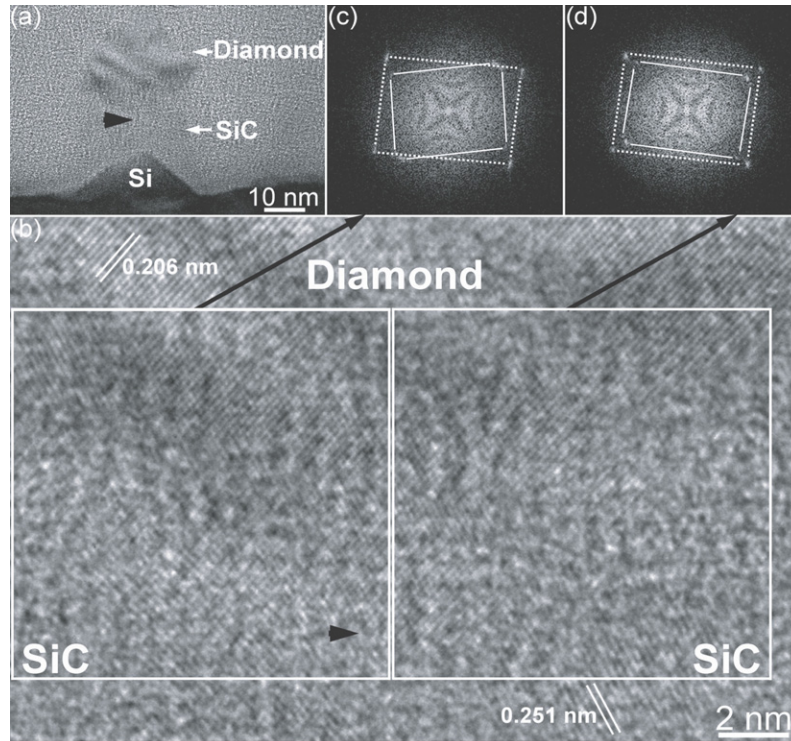
Figure 4. (a) HRTEM image of diamond on SiC. (b) Enlarged view of the region around the black arrow in (a). (c) and (d) FFT patterns from the white-framed regions on the left-hand and right-hand sides in (b), respectively, showing the orientation relationship between diamond and SiC.
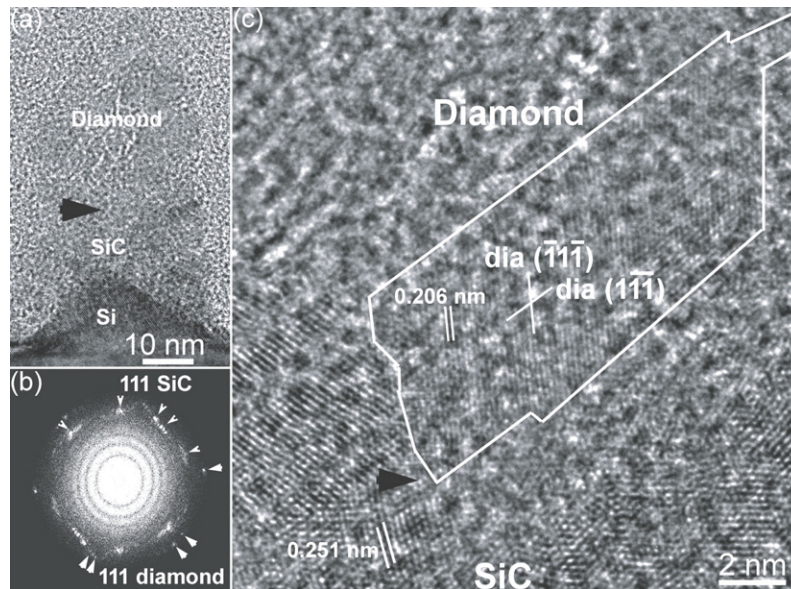

Figure 5. (a) HRTEM image from Si cones covered with multiple smaller secondary diamond particles. (b) FFT pattern from diamond and SiC region in (a). (c) An enlarged view of (a) around the black arrowed region, showing that there is only one diamond at the V-groove of SiC.

The SiC crystals are slightly misoriented to each other, similar to the previous cases. Figures 4(c) and (d) are FFT patterns from the white-framed regions on the left-hand and right-hand sides in figure 4(b), respectively. Examination of the lattice fringes and FFT patterns reveals that the diamond is actually epitaxial to the right-hand side SiC. The observation of the single diamond, in contact to the SiC groove, suggests that diamond nucleation is preferred at groove sites, similar to the case previously reported by Lee *et al* [28]. The groove provides a step for diamond nucleation, and the lateral growth direction for epitaxial diamond is likely to be along one of the SiC surfaces.

A typical HRTEM image from those Si cones covered with multiple smaller secondary diamond particles is shown in figure 5(a). The structure still consists of diamond, SiC and Si from its top to the base. Figure 5(b) is an FFT pattern from a region including SiC and diamond phases in figure 5(a). The diamond {111} reflections can be identified, revealing that the diamond is actually polycrystalline, with four crystallites in this case. Figure 5(c) is an enlarged view of figure 5(a) around the black arrow region. From the lattice fringes of the framed region, it can be concluded that there is only one diamond at the V-groove of SiC. This single diamond is also oriented with {111} planes parallel to {111}$_{SiC}$. Hence, it is suggested that this diamond is the first nucleus formed. The finding that a single-crystal diamond forms at the V-groove may have a significant implication for epitaxial growth, as it shows that nucleation of highly oriented diamond can be obtained in the very first stage of deposition. Secondary nucleation of diamond could be due to the uneven surface areas on the SiC, which increase with cone size. For better epitaxial growth of oriented diamond nanocrystals, therefore it is necessary to modify the experimental conditions soon after the oriented nucleation has completed, probably within a few tens of seconds to avoid secondary nucleation.

Based on the above results, it is clear that the nucleation of diamond on Si in the early stage of biasing is preceded by initially forming heteroepitaxial SiC layers on the Si cone with {111} facet steps, which then form a V-shaped groove after SiC growth and coalescence. The V-shaped groove provides the nucleation site for subsequent diamond formation as an epitaxial or oriented single diamond crystal. Without carefully controlled deposition conditions, secondary nucleation of diamond may take place.

4. Conclusions

In this study, nanometre-sized single-crystalline diamonds can be deposited by a short bias nucleation period using a microwave plasma CVD system with a dome-shaped Mo electrode. After the deposition, SEM and TEM analyses show that there is a high density of cones uniformly deposited on the surface of the substrate. TEM demonstrates that the cone-like structures are actually composed of conical Si crystals covered with nano-crystalline diamonds. Between Si and diamond, a thin layer of cubic SiC is found in epitaxy with Si. The growth of SiC on the opposite sides of the Si cone results in a V-groove which provides a favourable site for diamond nucleation. The consequently formed nanodiamonds are single crystalline, with a rhombus-like shape oriented along the Si[100] direction and in epitaxy with SiC.

References

[1] Angus J C and Hayman C C 1998 *Science* **241** 913
[2] Yang W S, Auciello O, Butler J E, Cai W, Carlisle J A and Gerbi J 2002 *Nat. Mater.* **1** 253
[3] Jan I, Johan H, Erik J, Tobias W, Daniel J T and Andrew J W 2002 *Science* **297** 1670
[4] Brus L E 1994 *Phys. Chem.* **98** 3575
[5] Rupp J and Birringer R 1987 *Phys. Rev.* B **36** 7888
[6] Gleiter H 1989 *Prog. Mater. Sci.* **33** 223
[7] Gruen D M, Liu S, Krauss A R, Luo J and Pan X 1994 *Appl. Phys. Lett.* **64** 1502
[8] Gruen D M, Liu S, Krauss A R and Pan X 1994 *J. Appl. Phys.* **75** 1758
[9] Wang S G, Zhang Q, Yoon S F, Ahn J, Wang Q, Yang D J, Zhou Q and Huang Q F 2002 *Mater. Lett.* **56** 948
[10] Jiang X and Jia C L 2002 *Appl. Phys. Lett.* **80** 2269
[11] Ding M Q, Choi W B, Myers A F, Sharma A K, Narayan J, Cuomo J J and Hren J J 1997 *Surf. Coat. Technol.* **94** 672
[12] Kurtsiefer C, Mayer S, Zarda P and Weinfurter H 2000 *Phys. Rev. Lett.* **85** 290
[13] Beveratos A, Brouri R, Gacoin T, Villing A, Poizat J P and Grangier P 2002 *Phys. Rev. Lett.* **89** 187901
[14] Brouri R, Beveratos A, Poizat J-P and Grangier P 2000 *Opt. Lett.* **25** 1294
[15] Jelezko F, Gaebel T, Popa I, Domhan M, Gruber A and Wrachtrup J 2004 *Phys. Rev. Lett.* **93** 130501
[16] Zhou X T, Li Q, Meng F Y, Bello I, Lee C S, Lee S T and Liftshitz Y 2002 *Appl. Phys. Lett.* **80** 3307
[17] Shechtman D, Feldman A, Vaudin M D and Hutchison J H 1993 *Appl. Phys. Lett.* **62** 487
[18] Dorignac D, Serin V, Delclos S, Phillipp F, Rats D and Vandenbulcke L 1997 *Diamond Relat. Mater.* **6** 758
[19] Yugo S, Kanai T, Kimura T and Muto T 1991 *Appl. Phys. Lett.* **58** 1036
[20] Stoner B R, Ma G H, Wolter S D and Glass J T 1992 *Phys. Rev.* B **45** 11067
[21] Jiang X, Klages C P, Zachai R, Hartweg M and Füsser H J 1993 *Appl. Phys. Lett.* **62** 3438
[22] Choi I H, Barrat S and Bauer-Grosse E 2003 *Diamond Relat. Mater.* **12** 361
[23] Barrat S, Saada S, Dieguez I and Bauer-Grosse E 1998 *J. Appl. Phys.* **84** 1870
[24] Schreck M, Baur T and Stritzker B 1995 *Diamond Relat. Mater.* **4** 553
[25] Kulisch W, Ackermann L and Sobisch B 1996 *Phys. Status Solidi* a **154** 155
[26] Stöckel R, Janischowsky K, Rohmfeld S, Ristein J, Hundhausen M and Ley L 1996 *Diamond Relat. Mater.* **5** 321
[27] Yan J K and Chang L 2006 *Thin Solid Films* **498** 230
[28] Lee S T, Peng H Y, Zhou X T, Wang N, Lee C S, Bello I and Lifshitz Y 2000 *Science* **287** 104